PRECIPITATION PROCESSES IN Al-4Cu-(0.3Mg, 0.5Cd) WT. % ALLOYS

B. T . Sofyan and S.P. Ringer*

School of Physics and Materials Engineering, P.O. Box 69M, Monash University, VIC, 3800 and * Australian Key Centre for Microscopy & Microanalysis, The University of Sydney, NSW, 2006, Australia

Trace additions of Cd, Sn and In to Al-Cu alloys are known to promote a fine and uniform dispersion of θ' (Al_2Cu, *I4/mcm*, *a*=0.404 nm and *c*=0.580 nm) and cause an increased hardening response. Although various mechanisms have been proposed for this effect, one-dimensional atom probe (1DAP) experiments on an Al-1.7Cu-0.01Sn (at. %) alloy have shown that θ' nucleation is preceded by clustering of Sn atoms and the precipitation of β-Sn[1]. The fine and uniform dispersion of θ' precipitates occurs subsequently such that the incoherent rim of the precipitates is associated with Sn atoms. Additions of Mg to Al-4Cu alloys promote the S phase (Al_2CuMg, *Cmcm*, *a*=0.404 nm, *b*=0.925 nm and *c*=0.718 nm) on $\{120\}_\alpha$ planes and recent 1DAP has shown that Mg-Cu co-clusters predominate during the early stages of ageing in ternary Al-Cu-Mg alloys [6]. The present work examines the effects of additions of Cd and Mg, both individually and in combination, on the precipitation processes in Al-4Cu (wt. %) alloys aged at 200 °C. An energy compensated three-dimensional atom probe (3DAP) has been used in conjunction with analytical transmission electron microscopy (TEM) to examine the precipitation process in general and, in particular, the nucleation of the strengthening phases.

Bright field (BF) TEM images of the peak hardness microstructure for each alloy during ageing at 200 °C were recorded close to the $<001>_\alpha$ zone axis and examples are provided in Fig. 1. The Al-Cu-Mg alloy microstructure is dominated by coarse θ', Fig.1 (a). The corresponding SAED pattern shows reflections at $\{110\}_\alpha$ positions and sharp streaks emerge from those positions parallel to the $<001>_\alpha$ direction, which are effects consistent with θ' phase. Fig. 1 (b) indicates that the peak hardness microstructure of the Al-Cu-Cd alloy consists of a dense and uniform distribution of θ' precipitates, together with a fine dispersion of smaller precipitates. Some of the small precipitates, which were identified as elemental Cd, remain independently in the α-matrix and some attach to the rim of the θ' phase. The peak hardness microstructure of the quaternary Al-Cu-Mg-Cd alloy consists mainly of the θ' and σ ($Al_5Cu_6Mg_2$, *Pm3*, *a* = 0.831 nm) phases (Fig. 3(c)). In addition, occasional Ω precipitates (Al_2Cu, *Fmmm*, *a*=0.496 nm, *b*=0.859 nm and *c*=0.848 nm) on $\{111\}_\alpha$ were also observed, inclined to the beam direction. Some S phase (Al_2CuMg, *Cmcm*, *a*=0.404 nm, *b*=0.925 nm and *c*=0.718 nm) precipitates were also detected. Careful inspection of the BF TEM images revealed that there were also small precipitates attached to both the θ' and σ phases. These particles were usually located on the edges or corners of the plate-like precipitates (arrowed). As with the Al-Cu-Cd alloy, a dispersion of small spheroidal precipitates was also observed, uniformly throughout the matrix.

A $<001>_\alpha$ DF STEM image of the θ'/spheroid/α region is provided in Fig. 2. Careful EDXS using a VG STEM revealed that the spheroids were Mg-Cd rich. This was different to the elemental Cd found to precipitate in the matrix and with θ' in the ternary Al-Cu-Cd alloy. The 3DAP was used to examine the pre-precipitate solute-solute

interactions and results are provided in Fig. 2(c-f). A preferred Cd-Mg interaction occurs. Significantly, the clustering of these atomic species facilitates the nucleation not only of θ', but also of σ and Ω. Although the mechanism of nucleation is thought to be the same for the Al-Cu-(Mg, Cd) alloys studied, the mixed chemistry of the clustering in the latter case allows the co-nucleation of several Al-Cu and Al-Cu-Mg based precipitates.

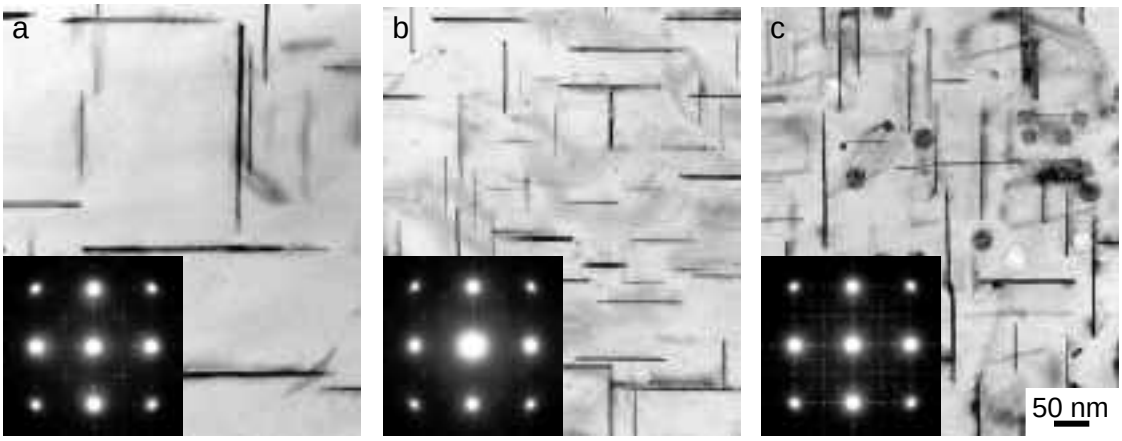

Figure 1. Peak hardness microstructures and SAED patterns of (a) Al-Cu-Mg; (b) Al-Cu-Cd and (c) Al-Cu-Mg-Cd alloys. BF TEM images with the electron beam near to $<001>_{\alpha}$.

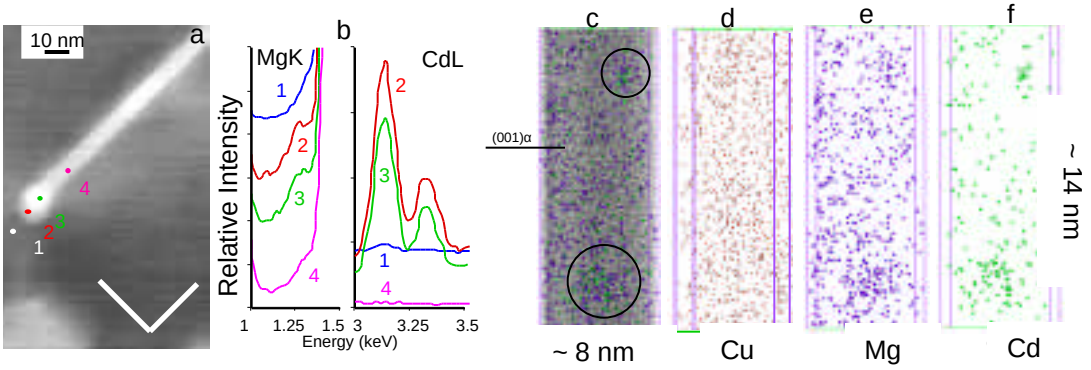

Figure 2. (a) $<001>_{\alpha}$ DF STEM image of typical θ' in the peak hardness microstructure of the Al-Cu-Mg-Cd alloy with the Mg and Cd EDXS profile from the points 1-4, indicated. The cube traces are marked in (a). (c-f): 3DAP elemental mapping of Al-Cu-Mg-Cd alloy aged at 200 °C, 15 min showing the presence of two clusters. Maps for (c) all atoms (d) Cu (e) Mg and (f) Cd atoms.

References

1. Ringer, S.P., K. Hono, and T. Sakurai (1995) Metall. Mater. Trans. A, 26A, 2207.

simon.ringer@emu.usyd.edu.au